AD-A020 940

RESISTANCE OF DIFFUSION-BONDED ELECTROLESS NICKEL-PLATED Ti-5Al-2.5Sn ALLOY TO HOT SALT STRESS CORROSION CRACKING

Anthony K. Wong, et al

Army Materials and Mechanics Research Center

Prepared for:

Army Materiel Command

December 1975

058158

AMMRC TR 75-26

AD

ADA020940

RESISTANCE OF DIFFUSION-BONDED ELECTROLESS NICKEL-PLATED Ti-5Al-2.5Sn ALLOY TO HOT SALT STRESS CORROSION CRACKING

ANTHONY K. WONG, MILTON LEVY, and JOSEPH L. MORROSSI
METALS RESEARCH DIVISION

D D C
FEB 20 1976

December 1975

Approved for public release; distribution unlimited.

ARMY MATERIALS AND MECHANICS RESEARCH CENTER
Watertown, Massachusetts 02172

The findings in this report are not to be construed as an official Department of the Army position, unless so designated by other authorized documents.

Mention of any trade names or manufacturers in this report shall not be construed as advertising nor as an official indorsement or approval of such products or companies by the United States Government.

UNCLASSIFIED

SECURITY CLASSIFICATION OF THIS PAGE (When Data Entered)

REPORT DOCUMENTATION PAGE		READ INSTRUCTIONS BEFORE COMPLETING FORM
1. REPORT NUMBER: AMMRC TR 75-26	2. GOVT ACCESSION NO.	3. RECIPIENT'S CATALOG NUMBER
4. TITLE (and Subtitle): RESISTANCE OF DIFFUSION-BONDED ELECTROLESS NICKEL-PLATED Ti-5Al-2.5Sn ALLOY TO HOT SALT STRESS CORROSION CRACKING		5. TYPE OF REPORT & PERIOD COVERED: Final Report 6. PERFORMING ORG. REPORT NUMBER
7. AUTHOR(s): Anthony K. Wong, Milton Levy, and Joseph L. Morrossi		8. CONTRACT OR GRANT NUMBER(s)
9. PERFORMING ORGANIZATION NAME AND ADDRESS: Army Materials and Mechanics Research Center, Watertown, Massachusetts 02172, AMXMR-EH		10. PROGRAM ELEMENT, PROJECT, TASK AREA & WORK UNIT NUMBERS: D/A Project: 1T162105AH84; AMCMS Code: 612105.11.H84; Agency Accession: DA 0B4762
11. CONTROLLING OFFICE NAME AND ADDRESS: U. S. Army Materiel Command, Alexandria, Virginia 22333		12. REPORT DATE: December 1975 13. NUMBER OF PAGES: 24
14. MONITORING AGENCY NAME & ADDRESS(if different from Controlling Office)		15. SECURITY CLASS. (of this report): Unclassified 15a. DECLASSIFICATION/DOWNGRADING SCHEDULE

16. DISTRIBUTION STATEMENT (of this Report)

Approved for public release; distribution unlimited.

17. DISTRIBUTION STATEMENT (of the abstract entered in Block 20, if different from Report)

18. SUPPLEMENTARY NOTES

19. KEY WORDS (Continue on reverse side if necessary and identify by block number)

Stress corrosion — Electroless nickel
Titanium alloys — Bent-beam test
Protective coatings — High temperature tests

20. ABSTRACT (Continue on reverse side if necessary and identify by block number)

(SEE REVERSE SIDE)

DD FORM 1 JAN 73 1473 EDITION OF 1 NOV 65 IS OBSOLETE

UNCLASSIFIED

SECURITY CLASSIFICATION OF THIS PAGE (When Data Entered)

Block No. 20

ABSTRACT

Bent-beam, constant deflection experiments at a temperature of 900 F for time durations up to 1000 hours indicated that diffusion-bonded (950 F or 1150 F in vacuum) electroless nickel plate was affected by hot salt stress corrosion (HSSC). However, the protective plate demonstrated potential for reducing the susceptibility of the Ti-5Al-2.5Sn titanium alloy substrate to HSSC cracking. Mechanically induced surface defects (indentations, scratches) in the surface of the plate did not significantly alter the patterns of corrosion attack. Continued in-house efforts to establish failure mechanisms and to optimize plating processes are contingent upon results from further tests to determine erosion and fatigue behavior of these materials at elevated temperatures. (Authors)

CONTENTS

INTRODUCTION

Numerous laboratory experiments[1] have verified the susceptibility of titanium alloys to embrittlement and cracking under tensile loading at elevated temperatures greater than 400 F in the presence of halides. Since titanium alloy gas turbine compressor components in military aircraft, such as rotor blades and centrifugal impellers, may be exposed simultaneously to high operating temperatures and salt-laden air environments, catastrophic failure of aircraft engines remains a definite hazard. Although there exists a paucity of recognized failures attributed to hot salt stress corrosion cracking (HSSCC), one field service report* identified the damage to a titanium disk in the compressor section of a Navy TF30 aircraft engine as being caused by the HSSCC phenomena. Unfortunately, the susceptibility of titanium alloy components to HSSCC can be expected to increase with the increasing operating temperatures proposed for the compressor section of advanced gas turbine engines.

A review of Army overhaul records[2] reveals that sand and dust erosion damage, along with foreign object damage, are among the leading causes of premature engine removals from helicopters. Erosion of compressor components is a well-recognized reliability and maintainability (R&M) problem which serves to increase unscheduled engine replacement (UER), accidents, and maintenance man-hour (MMH) rates. Protective coatings have been suggested by many investigators as one of several promising means to alleviate the erosion problem.

Earlier research studies[3,4,5] have demonstrated that diffusion bonding of electroless nickel plate is a satisfactory technique for producing a wear-resistant surface on titanium alloys at room temperature. However, further studies are needed to validate the potential of electroless nickel plate against both erosion and salt stress corrosion at higher temperatures.

For this investigation, an exploratory study was made of diffusion-bonded electroless nickel plates for reducing the susceptibility of titanium alloys to HSSCC. A test temperature of 800 F was selected as representative of a high operating temperature projected for the compressor section of advanced high-performance aircraft engines.

TEST MATERIALS

Ti-5Al-2.5Sn Alloy

An alpha-type 5Al-2.5Sn titanium alloy with a nominal sheet thickness of 1/32 inch was used in this study. This alloy is a weldable grade which normally

*Private Communication: Mr. S. Goldberg, Naval Air Systems Command, 5 December 1972.

1. RIDEOUT, S. P. *The Initiation of Hot-Salt Stress Corrosion Cracking of Titanium Alloys* in Applications Related Phenomena in Titanium Alloys, ASTM STP 432, American Society for Testing and Materials, 1968, p. 205-217.
2. RUMMEL, K. G., and SMITH, H. J. M. *Investigation and Analysis of Reliability and Maintainability Problems Associated with Army Aircraft Engines.* US Army Air Mobility Research and Development Laboratory, USAAMRDL Technical Report 73-28, August 1973.
3. LEVY, M., and ROMOLO, J. *Improved Adhesion of Electroless Nickel Plating on Titanium Alloys.* 48th Annual Technical Proceedings Am. Electroplaters Soc., 1961, p. 135-141.
4. KOSTMAN, S. J. *Lubricants and Wear Coatings for Titanium* in Applications Related Phenomena in Titanium Alloys, ASTM STP 432, American Society for Testing and Materials, 1968, p. 268-282.
5. LEVY, M., and MORROSSI, J. L. *Wear- and Erosion-Resistant Coatings for Titanium Alloys in Army Aircraft.* Army Materials and Mechanics Research Center, AMMRC TR 70-36, December 1970.

possesses good oxidation resistance, stability, and strength at elevated temperatures and thus is a candidate material for structural applications at high temperatures.

Composition of the test alloy, shown by the manufacturer's data in Table 1, was within the limits specified by ASTM B265-58T, grade 6. Mechanical property measurements indicated that the hardness of this mill-annealed sheet was R_c 35. This information along with tensile properties data as a function of rolling direction is shown in Table 2. It may be noted that the strengths and ductility were somewhat higher in the longitudinal direction.

Electroless Nickel Plating

To determine the efficacy of diffusion-bonded electroless nickel plates in protecting titanium alloy substrates from HSSCC, Ti-5Al-2.5Sn alloy sheet specimens about 3/8 inch wide and 6 inches long, in the mill-annealed condition, were processed with a plating thickness of approximately 0.6 mil. This electroless nickel plating was produced through the selective deposition of a high nickel, low phosphorous alloy onto the solid catalytic surface by means of chemical reduction of a nickel salt with sodium hypophosphite. The electroless nickel plate is usually 93 to 95% nickel; the remainder is primarily phosphorous, probably nickel phosphide. Specimen preparation and plating procedures utilized were modifications of the techniques employed in a past study[5] of wear-resistant coatings on titanium.

Enhancement of the hardness and bonding characteristics were promoted by thermal diffusion treatments in a vacua for 4 hours. It is also common practice to heat treat as-deposited electroless nickel plates at temperatures above 750 F to increase as-plated hardness and to decrease inherent brittleness. Within limits, the hardness decreases with further increases in treatment temperatures.

One group of specimens was diffusion treated in a 950 F environment, while the other group was exposed to an 1150 F diffusion environment. These treatments decreased the hardness of the titanium substrate from R_c 35 to R_c 29. However, as indicated by the data in Table 3, the hardness of the 950 F diffusion-treated nickel coating was as high as R_c 39, whereas the higher temperature treatment resulted in a lower coating hardness of only R_c 34. The original measurements were made with Knoop indenters. Hence, the Rockwell hardness values cited herein are converted numbers which, at best, are only approximate values which can reasonably be used only to establish relative ranking of hardness.

Metallographic examination of selected cross-sections of the diffusion-treated specimens revealed no appreciable differences in the microstructures of

Table 1. CHEMICAL ANALYSIS OF Ti-5Al-2.5Sn ALLOY SHEET

Composition (wt. %)

Al	Sn	Fe	C	N	Mn	Ti
5.4	2.5	0.35	0.02	0.015	0.01	Bal

Table 2. MECHANICAL PROPERTIES OF Ti-5Al-2.5Sn ALLOY SHEET

Orientation	U.T.S. (ksi)	Y.S. (0.2% offset) (ksi)	Elon. (%)	R.A. (%)	Hardness (R_c)
Transverse	129.0	123.0	15.5	34.7	35
Longitudinal	136.0	129.7	16.5	42.5	35

Table 3. HARDNESS OF ELECTROLESS NICKEL-PLATED SPECIMENS

Ti-5Al-2.5Sn Substrate	Hardness Measured	R_c*	DPN*
950 F to 1150 F Treatment	KHN_{500} 312	29	300
As-received	KHN_{500} 350	35	350
Electroless Nickel Coatings			
1150 F Treatment	KHN_{25} 460	34	340
950 F Treatment	KHN_{25} 525	39	380

*Approximate values based on conversion tables: Metals Progress Data Sheet, September 1958, pg. 96-B, and ASM Metals Handbook, 1961, pg. 1234.

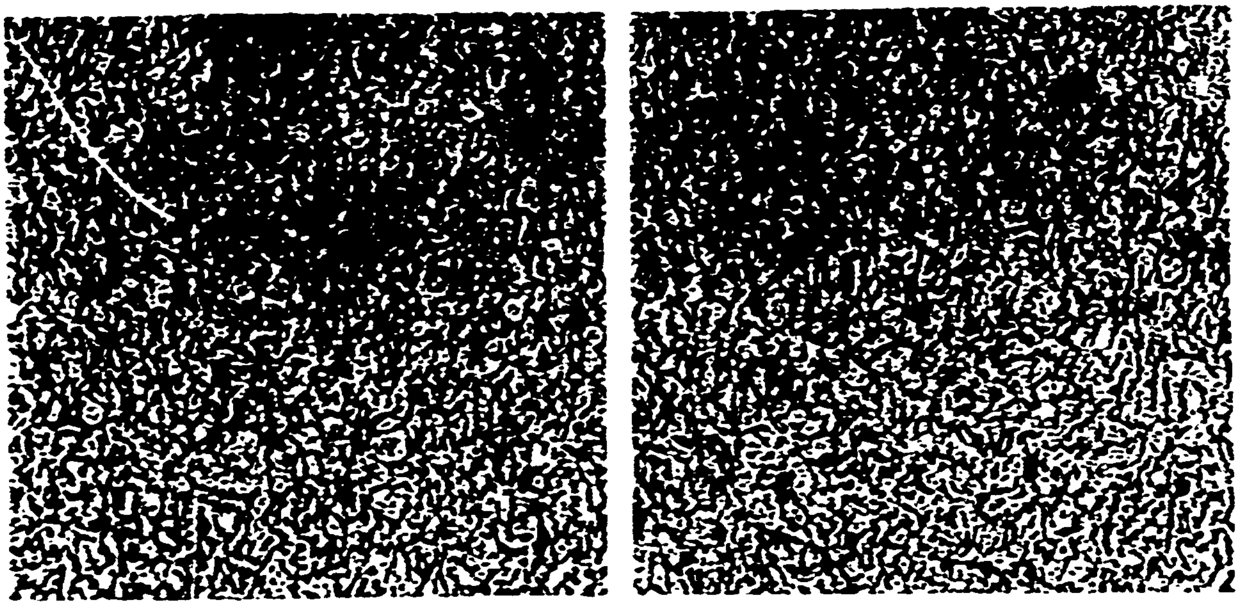

a. 950 F - 4 hours - in vacuum

b. 1150 F - 4 hours - in vacuum

Figure 1. Microstructure of Ti-5Al-2.5Sn alloy after diffusion heat treatment. Mag. 200X

the substrates, as shown by two representative photomicrographs in Figure 1. The etchant used in preparing both specimens for examination was a 2% HF solution. In addition, hardness tests indicated no measurable effects attributable to the two different exposure temperatures.

In the as-plated condition, adhesion of the plating was relatively poor. Adhesion is known to be enhanced by high diffusion temperatures, manifested by metallurgical bonding at temperatures as low as 750 F.[3,5] The photomicrograph in Figure 2a shows the appearance of the cross-section of the coating and substrate heat treated at 950 F. X-ray diffraction analyses of plated Ti-8Al-1Mo-1V and Ti-6Al-6V-2Sn alloys in an earlier experiment[5] indicated that diffusion between the coating and substrate does indeed occur at 950 F for these alloys. Thus, although not evident in Figure 2a, there is reason to believe diffusion and the formation of intermetallics also occurred with the Ti-5Al-2.5Sn alloy. The presence of a clearly defined diffusion layer was more evident after the 1150 F heat treatment as shown by Figure 2b. Measurements revealed that the thickness of the plating varied between 0.5 to 0.7 mil, averaging about 0.6 mil.

a. Diffusion treatment: 950 F in vacuum - 4 hours. b. Diffusion treatment: 1150 F in vacuum - 4 hours.

Figure 2. Electroless nickel plating on Ti-5Al-2.5Sn substrate. Mag. 1000X

Test Specimen

Strip specimens were cut and ground to finish dimensions of 3/8 inch wide by 6 inches long from a 1/32-inch mill-annealed Ti-5Al-2.5Sn alloy sheet. Figure 3 shows this specimen. The ends were ground to be at right angles to the specimen length and the sharp corners removed. To investigate effects of specimen orientation, some of the strips were cut with their lengths parallel to the rolling direction of the sheet and are herein referred to as longitudinal specimens. Transverse specimens were cut with the length perpendicular to the rolling direction.

For the study of the efficacy of electroless nickel plating against HSSCC, one group of titanium specimens was processed on all sides with the plating. As mentioned in the previous section, some of the plated specimens were diffusion treated in vacua at 950 F, while the remainder were treated at 1150 F. However, for control purposes, another group of noncoated titanium specimens was also exposed to the aforementioned heat treatments. In addition, some specimens were reserved for testing in the as-received mill-annealed condition. Table 4 summarizes the orientation and plating condition of the various test specimens.

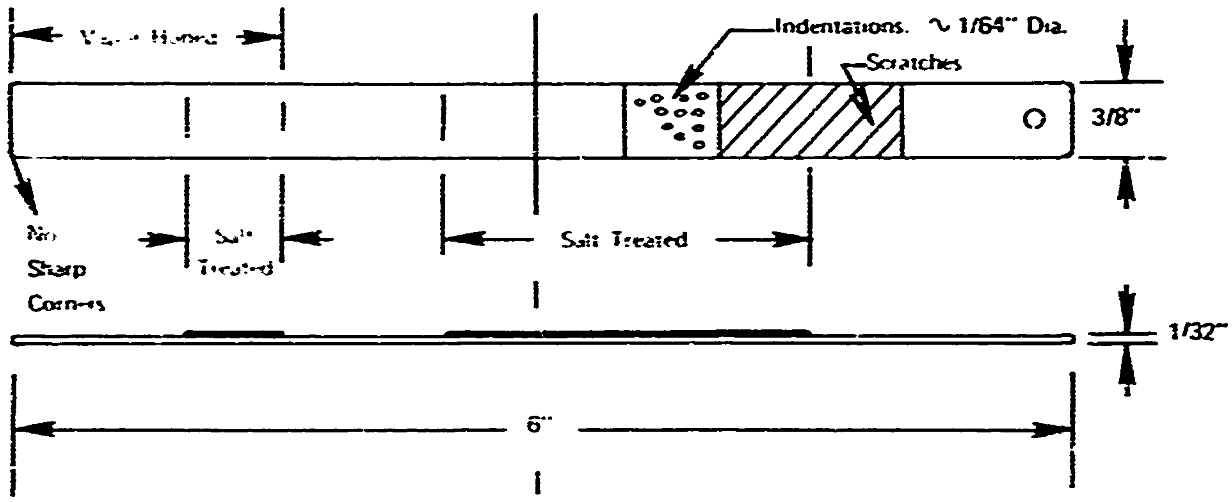

Note: Electroless Nickel Plate Thickness ∿ 0.6 mil

Figure 3. Constant deflection bent-beam specimen.

Table 4. HSCC BENT-BEAM TEST SPECIMENS
(900 F - 50 ksi Initial Stress)

Spec.	Plated	Heat Treat (deg F)	Orient.	Test Duration (hours)	Note
A1	No	*	L	150	Through Fracture
N1	Yes	950	L		
E1	Yes	1150	L		
A2	No	*	T		Near Fracture
N2	Yes	950	T		
E2	Yes	1150	T		
A3	No	*	L	500	
N3	Yes	950	L		
E3	Yes	1150	L		
A4	No	*	T		
A5	No	*	L	1000	
N5	Yes	950	L		
E5	Yes	1150	L		
A7	No	950	L		
E7	No	1150	L		Through Fracture
A6	No	*	T		
N6	Yes	950	T		Near Fracture
E6	Yes	1150	T		
A8	No	950	T		Through Fracture
E8	No	1150	T		Through Fracture

*As-received mill-anneal condition

TEST PROCEDURE

General Test Approach

In this study, constant deflection bent-beam specimens were mounted in AMMRC-modified[5] Pratt and Whitney type test fixtures. These fixtures were

subsequently loaded into a muffle-type, electric furnace and exposed to an ambient temperature of 900 F, in quiescent air, for durations up to 1000 hours. All of the flexed specimens were treated with salt deposits on selected areas of the convex (tension) surface. Specimen test variables included noncoated and electroless nickel-plated titanium, two diffusion treatment temperatures, sheet orientation, and mechanically induced surface defects to simulate accidental surface damage. Post-test evaluation was limited to metallographic examinations of the surface damage and cracks attributable to hot salt stress corrosion.

Specimen Preparation

Since mechanical defects on the surface of stressed components could conceivably influence the mechanisms operating to produce HSSCC because of the presence of stress raisers, a limited attempt was made to monitor the phenomena. As indicated in Figure 3, a section of the electroless nickel-plated specimen was scratched with a tungsten carbide scribe to produce randomly spaced grooves aligned 45° to the direction of stress on the surface. Microscopic examination revealed that the grooving action removed some of the coating. The depth of the groove was less than 1/2 mil. There were no signs of the substrate being exposed. In addition, an automatic hand center punch, with a 90° cone angle indenter, was used to produce random indentations in the coating surface to a depth of about 1 mil. Although the electroless nickel plating was only about 0.6-mil thick, it appeared to be plastically deformed into the cavity without exposing the substrate.

In preparation for the salt treatment, the specimens were lightly wiped with fine emery cloth, washed in an alkaline bath, cleaned with acetone (reagent grade), and then rinsed in distilled water. A small section of the coating was also cleaned by a wet abrasive blast (vapor honing) method to assess the need for additional surface preparation. As will be shown later, this latter method does indeed provide a surface which promotes a more uniform distribution of the precipitated salt particles.

A 3% sodium chloride solution was applied to selected areas of each coated specimen somewhat as shown in Figure 3. The solution was spread evenly over the surfaces. The specimen was then placed on a hot plate, set at temperature of about 180 F, and held at that heat level while the water in the saline solution slowly evaporated, leaving behind a dry, white, translucent residue. Also as shown in Figure 3, the salt-treated sections encompassed a portion of the vapor-honed area, the mid-length area of the specimen, and the regions containing mechanically induced indentations and scratches. Other sections were left untreated as test controls.

Weight measurements indicated that the areal density of the dry salt deposit was about 10 milligrams per square inch. This quantity of salt is almost double the amount of dry salt actually found to be deposited on a select group of aircraft engine components after flight operations.[7] Although it appears, as a first approximation, that increased quantities of deposited salt represents a more severe HSSCC condition, the hypothesis remains unverified. However, under

6. WONG, A. K., and LEVY, M. *Hot Salt Stress Corrosion of Titanium Alloys in an Adjustable Deflection, Multi-Specimen Bent Beam Test Apparatus.* Army Materials and Mechanics Research Center, AMMRC TR 73-10, March 1973.

7. ASHBROOK, R. L. *A Survey of Salt Deposits in Compressors of Flight Gas Turbine Engines.* National Aeronautics and Space Administration, Report No. TN D-4999, January 1969.

some condition of moisture content, salt precipitate configuration, temperature, gas velocity, and pressure, etc., the stress corrosion of titanium can be expected to increase with increasing areal density of salt up to some undetermined limit. Further increases in areal density may cause a reverse effect.

Hot Salt Stress Corrosion Test

Following salt treatment, the specimens were carefully flexed and inserted into the bent-beam test fixture which was set to a predetermined span length. Although the ends of the specimens were ground to be perpendicular to the specimen length and the specimen ends rounded, extra effort was made to properly align the specimens relative to the end restraints to minimize undesirable stresses. An earlier report[6] describes the fixture and test procedures in greater detail.

Static surface stresses in a rectangular beam of finite length with a fixed deflection are strongly dependent upon the length and thickness of the structure. Figure 4 shows an illustration of a bent beam held in place by end restraints to maintain a fixed deflection span. Using an exact elastic stress analysis method proposed by Loginow et al.[8,9], calculations were made to establish a specimen length and deflection which would effectively generate a maximum tensile stress of 50 ksi, at 900 F in a sheet 1/32 inch thick. This maximum tensile fiber stress was determined from the following relationship:

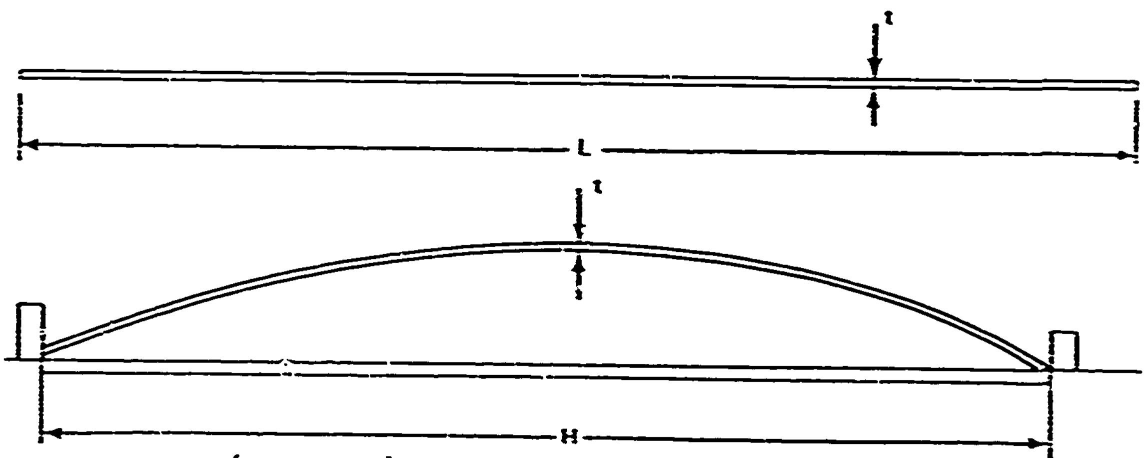

$$\sigma = 4E_m \left\{ 2E(k) - K(k) \right\} \left\{ \frac{k}{2} - \frac{2E(k) - K(k)}{12} \left(\frac{t}{H} \right) \right\} \frac{t}{H}$$

$$\text{and } L = H \left\{ \frac{2\left[K(k) - E(k) \right]}{2E(k) - K(k)} + 1 \right\}$$

Loginow et al. (Ref. 8, 9)

Figure 4. Stressing of bent-beam test specimen.

8. PHILLIPS, L. H., and LOGINOW, A. W. *Stress Corrosion of Steels for Aircraft and Missiles.* Corrosion-National Association of Corrosion Engineers, v. 16, Feb 1960, p. 97.
9. HAAIJER, G., and LOGINOW, A. W. *Stress Analysis of Bent-Beam Stress Corrosion Specimens.* Corrosion-National Association of Corrosion Engineers, v. 21, no. 4, April 1965.

$$\sigma = 4E_m \, [2E(k) - K(k)] \, [k/2 - \frac{2E(k) - K(k)}{12} (t/H)] \, t/H$$

wherein K(k) and E(k) are the complete elliptical integrals of the first and second kind, respectively, and k is the modulus of these integrals. Further, σ is the maximum tensile strength, E_m is Young's modulus, t is the specimen thickness, and H is the distance between the two ends of the deflected specimen as shown in Figure 4. Additionally, the length of the specimen L was derived from the following ratio:

$$\frac{L-H}{H} = \frac{2[K(k) - E(k)]}{2E(k) - K(k)}$$

Assuming a high temperature Young's modulus of 11.6 x 10^5 psi, it was calculated that a specimen 6.0 inches long, deflected to a span length of 5.6 inches, would produce the prescribed stress condition. For more accurate determinations of prestresses, actual measured values of high temperature Young's moduli and effects of thermal expansion should be employed in the calculations.

It may be noted that the typical minimum yield strength of the Ti-5Al-2.5Sn alloy at 900 F should be in the vicinity of 57 ksi. Therefore, assuming no residual stress to be present, the experimental prestress of 50 ksi should not cause any appreciable initial yielding. However, related data further indicate that a tensile stress of only 48 ksi, at 800 F, will produce 1% creep in 100 hours. Consequently, in this fixed deflection test, relaxation of stresses due to creep will serve to reduce the initial prestress loading as the exposure time increases.

The fixtures loaded with specimens were placed into a large muffle furnace which was then heated up to 900 F. These stressed specimens were exposed, in quiescent air, to a constant furnace temperature of 900 F for a time duration of either 150, 500, or 1000 hours. Table 4 identifies the individual specimens and test parameters.

Post-Test Evaluation

Removal of the individual 150- and 500-hour test specimens at the scheduled time intervals was accomplished by employing long-handle tongs. The fixture itself remained in the furnace for the full 1000-hour duration of testing. Figure 5 is a photograph showing several plated and nonplated specimens in the test fixture shortly after removal from the furnace after exposure for 1000 hours. Upon separation from the test fixture, each specimen was visually examined for fractures and cracks. Subsequently, the specimens were cleaned of the salt residue and reaction products by means of wet abrasive blast techniques and re-examined at magnifications up to 20X. In order to fully appreciate the extent of damage to the surface, it was necessary to chemically etch the specimens. The coating on some specimens was mechanically removed to further investigate the damage to the substrate.

An etchant composed of 50 ml nitric acid, 10 ml hydrofluoric acid, and 10 ml sulfuric acid was used to reveal the cracks in the surface of the noncoated titanium specimens. The specimens were immersed in the acid solution for 60 seconds

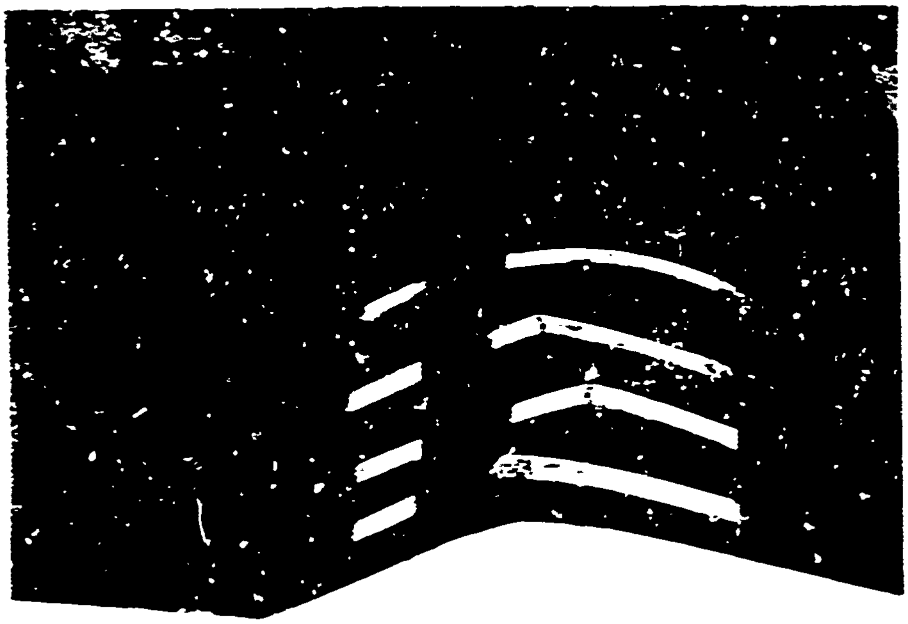

Figure 5. Plated and nonplated specimens in test fixture after heating at 900 F for 100 hours.

Spec. No.	
(N5)	Plated
(N6)	Plated
(E5)	Plated
(E6)	Plated
(N7)	Nonplated
(N8)	Nonplated
(E7)	Nonplated
(E8)	Nonplated

at room temperature or until excessive red fumes were liberated. An alternate method was to immerse the specimens for only 30 seconds at a solution temperature of 140 F. Similarly, a 2% HF solution was used to etch the electroless nickel coating for study. Photomacrographs were taken to record representative surface conditions. Kroll's reagent was also used to etch the titanium microstructure for general examinations of structure and cracks in the cross section.

RESULTS AND DISCUSSION

Initial Post-Exposure Inspection

After 150 hours at 900 F, the first group of longitudinal and transverse specimens, see Table 4, were removed from the fixture in the furnace and examined after cooling to room temperature. Damage to these specimens was not clearly evident because of the salt-encrusted surfaces. Figure 6 shows the top view of these curved specimens. As designated in the figure, only select areas of the specimens were salt-treated. A small portion of each specimen was left untreated to provide a basis for comparing damage due to HSSCC. As alluded to by the reflected highlights from the specimens shown in the figure, the nonsalted segments of the electroless nickel-coated specimens retained a metallic sheen. However, the exposure to high temperatures converted the original silver color to a light bronze tint. In marked contrast, the hot oxidizing furnace atmosphere changed the shiny surface of the unsalted, uncoated titanium specimens, Figure 6b, to a dull, blue-purple surface. Except for oxidation, no damage was observed on the nonsalt-treated sections of these specimens.

Also in marked contrast between the plated and nonplated specimens was the visual appearance of the salt and reaction products on the specimens, after removal

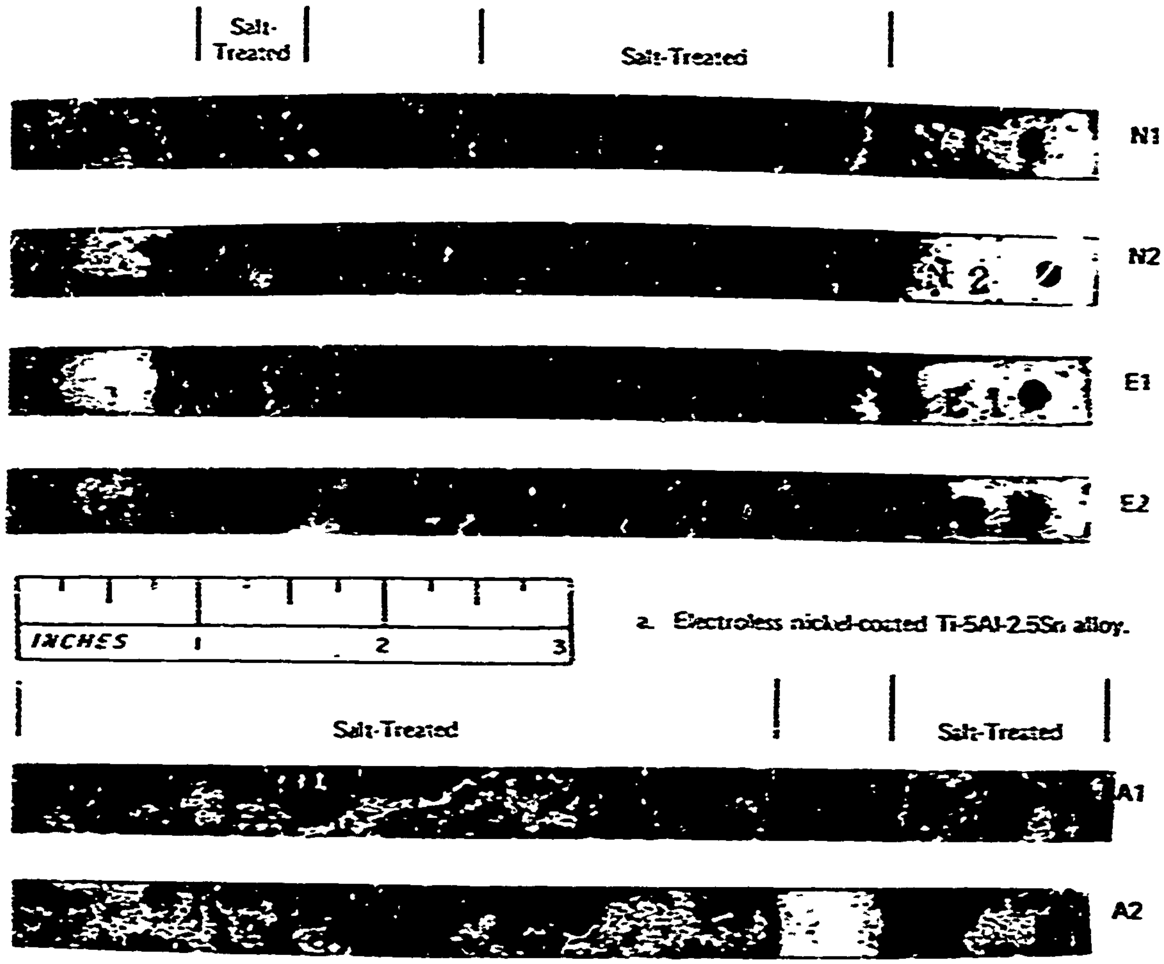

a. Electroless nickel-coated Ti-5Al-2.5Sn alloy.

b. Unplated Ti-5Al-2.5Sn alloy.

Figure 6. Specimens after removal from furnace after 150 hours at 900 F (top view).

19-066-1690/AMC-72

from the furnace. The residue on the electroless nickel-plated surfaces remained relatively translucent-white in tone and apparently changed only minimally. But on the bare titanium alloy, the salt and its reaction products expanded in volume, producing a thicker, rough layer, rusty-ivory in color on its outer periphery and graduating to varying shades of black at the approaches to the salt-metal interface. Another view of some salt-encrusted specimens after 1000-hour exposure was shown earlier in Figure 5. The four thickly coated specimens shown in the lower part of the test fixture represent salt treatments on nonplated titanium specimens. Specimen identification numbers listed may be coordinated with the data listed in Table 4.

Confirming the dissimilar characteristics of the salt reaction products was the observation that the residue on the plated surfaces was readily soluble in warm water, whereas the residue on the bare titanium alloy surfaces required the application of the more vigorous vapor blasting method to facilitate its removal. No attempt was made to analyze the reacted products. However, an earlier

investigator[16] reported that X-ray diffraction patterns of salt residue on titanium specimens exposed at 800 F for 64 days revealed the presence of anatase, rutile, sodium chloride, and an unidentified compound.

Surface preparation techniques play an important role in salt treatment of the test specimens. Examination of the photographs in Figure 6 reveals poor wettability and uneven precipitation of the salt deposits on some of the test segments. However, it may be noted in Figure 6a that the short, salt-treated segment on the left side of the specimens exhibited areas of uniform salt coating. These areas were vapor blasted before the salt treatment. Hence, vapor blasting techniques appear to be a desirable method for promoting wettability and uniform dispersion of salt particles. Consideration must be given to the fact that stresses imposed upon the specimens may be critical, particularly for thin sections.

General Modes of Hot Salt Corrosion Failure

Visual examination of the plated specimens, at higher magnification, after etching in an HF solution to enhance the presence of surface damage, revealed that hot salt did indeed corrode the diffusion-treated electroless nickel coatings. Evidence of pitting and general corrosion was discovered even on the compressive side of the specimen exposed to 900 F for 150 hours, indicating that tensile stress was not a necessary contributing factor. Troughs, strain lines, and a limited number of cracks, similar to the HSSCC damage occurring in unprotected titanium alloys, were additionally present on the tension-stressed plated surfaces. These in-line defects were oriented normal to the direction of tension loading, as expected.

Combinations of the aforementioned corrosion-induced defects were well-represented in the tension-stressed surface of plated specimen E6 after exposure to 900 F for 1000 hours. Areas damaged by hot salt attack are evident in the photograph of the specimen in Figure 7a. Swirl-like chains of corrosion pits

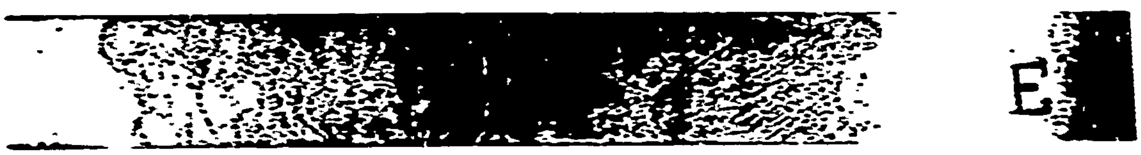

a. Specimen E6 - Electroless nickel plated surface.

b. Specimen E8 Nonplated Ti-5Al-2.5Sn alloy.

Figure 7. 1000 hour test at 900 F - 1150 F diffusion treatment - salt-treated transverse specimens - etched. Mag. 2X

16. LOGAN, H. L. Studies of Hot Salt Cracking of the Titanium 8Al-1Mo-1V Alloy. Proceedings of the Conference on Fundamental Aspects of Stress Corrosion Cracking, Ohio State University, 1967. Publication of National Association of Corrosion Engineers, 1969.

are attributable to the nonuniform precipitation of salt during the dehydration of the saline solution. Poor wettability also contributes to the uneven pattern of corrosion. Cracks in the surface are readily distinguished from the troughs by the width and contour of the gaps. It is suspected that the wider gap troughs were formed by the conjugation of corrosion pits which preferentially initiate along strain lines. Also, clearly shown in the same photograph are the mechanically induced punch marks; less evident are the diagonal scratch lines which appear to have been partially erased by the corrosion process. Some observations on the effects of interaction of the corrosion process with the mechanically induced defects will be made later in this report. A comparison of the salt-damaged surface of electroless nickel-plated specimen E6 may be made with the salt-damaged surface of nonplated titanium specimen E8, shown in Figure 7b, which was tested under equivalent conditions.

Effects of 150-Hour Exposure

Under the conditions prescribed for this experiment, unprotected Ti-5Al-2.5Sn alloys are susceptible to HSSCC. This phenomenon was verified by tests on non-plated control specimens A1 and A2, shown in Figures 8a and 8b. Oblique lighting was employed for the series of photographs in this figure, as well as in the next three figures, to highlight damaged areas. Under this lighting condition, defects penetrating into the surface such as cavities, scratches, pits, cracks, and troughs emerge as white forms on a black background. Table 4 summarizes the test parameters of the test specimens.

To a lesser degree, the hot salt also attacked the plated specimens, manifested by cracks, troughs, and pits, as shown in Figure 9. The induced scratches had only a nominal effect on the corrosion pattern. With respect to the punch marks, it was noted that occasional cracks and pits intersected the cavities with no positive signs of preferential attack. For example, in plated specimen X2, Figure 9c, troughs or cracks appear to interact with only two of the nine induced cavities. In specimen X1, Figure 9a, small pits exhibited even less corrosion attack about the indentations. Hence, the hot salt corrosion effects on accidental scratches and indentations in the plating was judged to be only minimal after exposure to 900 F for 150 hours.

Effects of 500-Hour Exposure

Hot salt stress corrosion cracking damage to titanium alloys increases with exposure time by the initiation of new cracks on the hydrogen-embrittled surface, conjoining of small cracks, and crack propagation. For baseline comparison, Figure 10a exhibits the multitudinous quantity of cracks in one salt-treated

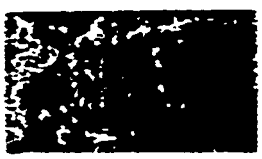

a. Annealed longitudinal specimen A1.

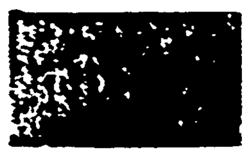

b. Annealed transverse specimen A2.

Figure 8. 150-hour test at 900 F - salt treated Ti-5Al-2.5Sn specimens - etched - oblique lighting. Mag. 2X

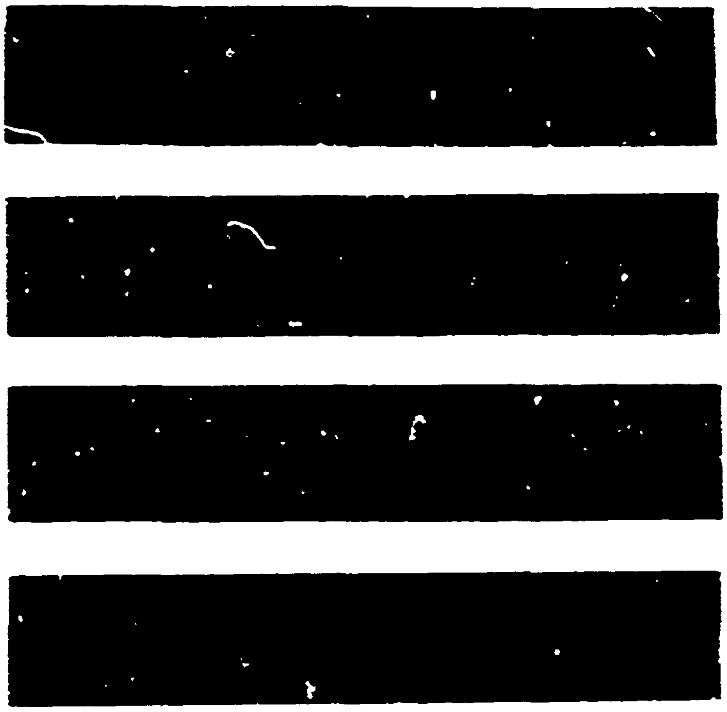

a. 950 F diffusion treatment - longitudinal specimen N1.

b. 1150 F diffusion treatment - longitudinal specimen E1.

c. 950 F diffusion treatment - transverse specimen N2.

d. 1150 F diffusion treatment - transverse specimen E2.

Figure 9. 150-hour test at 900 F - salt treated electroless nickel-plated Ti-5Al-2.5Sn specimens - etched - oblique lighting. Mag. 2X

segment of nonplated, longitudinal specimen A3 after 500 hours of exposure. Transverse specimen A4 (not shown) also encountered similar damage, indicating no effects attributable to specimen sheet orientation.

As expected, despite the decrement in surface tensile stresses due to creep, the increase in exposure time to 500 hours also increased the corrosion damage of the electroless nickel plate as demonstrated by specimens N3 and E3 in Figures 10b and 10c. Confirmation of this phenomenon may be made by comparing the corresponding specimens shown earlier in Figures 9a and 9b.

Moreover, at 500 hours distinctive patterns of surface failure modes emerged which were attributable to the two different diffusion treatment temperatures (950 F and 1150 F) employed to promote bonding of the nickel plate to the titanium substrate. For example, the presence of troughs with wider corrosion gaps were detected in the 950 F treated specimen N3, whereas an increase in the number of thin-line cracks in the 1150 F treated specimen E3 was observed. Furthermore, the cracks preferentially appeared in regions of higher stresses such as in the specimen edge and around the induced cavities. In the latter phenomenon, it may be speculated that the beneficial compressive stresses imposed by the mechanically induced punch marks were partially relieved by continued exposure at 900 F, thereby bequeathing a surface indentation which behaved as a stress raiser. Since no obvious damage appeared in the nonsalt-treated segments and since the troughs and cracks which appeared in the salt-treated segments were preferentially aligned normal (90°) to the direction of the applied tensile stress, it is concluded that the electroless nickel plating is indeed susceptible to hot salt stress corrosion.

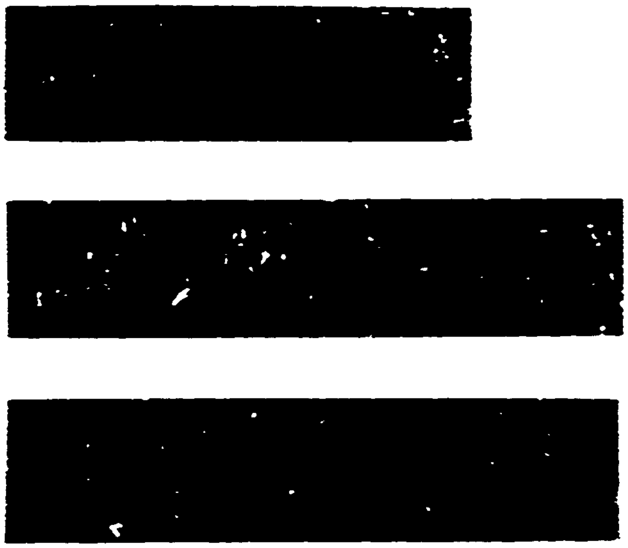

a. Annealed, uncoated
Ti-5Al-2.5Sn alloy specimen A3.

b. 950 F diffusion
treatment - electroless
nickel-plated specimen N3.

c. 1150 F diffusion
treatment - electroless
nickel-plated specimen E3.

Figure 10. 500-hour test at 900 F - salt-treated longitudinal specimens -
etched - oblique lighting. Mag. 2X

In the evaluation of the results, the mode and density of corrosion damage are more important factors than the actual fracture of a specimen since the fracture is generally manifested by the random and rapid joining of individual cracks followed by catastrophic failure.

Effects of 1000-Hour Exposure

Continued increases in exposure duration up to 1000 hours generated escalating corrosion attack to the salt-treated metal surfaces. Selected examples of these phenomena are clearly exhibited by the higher magnification photographs of three specimens in Figure 11 As alluded to in an earlier statement, in the experimental setup employed in this study only the test temperature and specimen deflection span are held constant. With the passage of time, relaxation of the tension surface, because of high temperature creep, effectively reduces the initial surface tensile stress of 50 ksi to only a small fraction of that value after 1000 hours. Moreover, the original salt deposits have been or continue to be consumed by the ongoing chemical reactions. The general aspect of some plated and nonplated specimens as they appeared in the test fixture after exposure for 1000 hours was shown earlier in Figure 5. At this exposure duration, the nonsalt-treated segments appeared to be quite undamaged, with oxidized surface film colors of golden bronze for the nickel-plated specimens and dark metallic blue for the nonplated specimens.

Inspection of corresponding photographs of test specimen surfaces after 150 and 500 hours of exposure at 900 F in Figures 9 and 10 with the 1000-hour effects depicted in Figure 11 reveals the progressive nature of the salt attack on the diffusion-bonded electroless nickel plate, manifested by the proliferation and growth of corrosion pits, troughs, and cracks as influenced by prolonged exposure

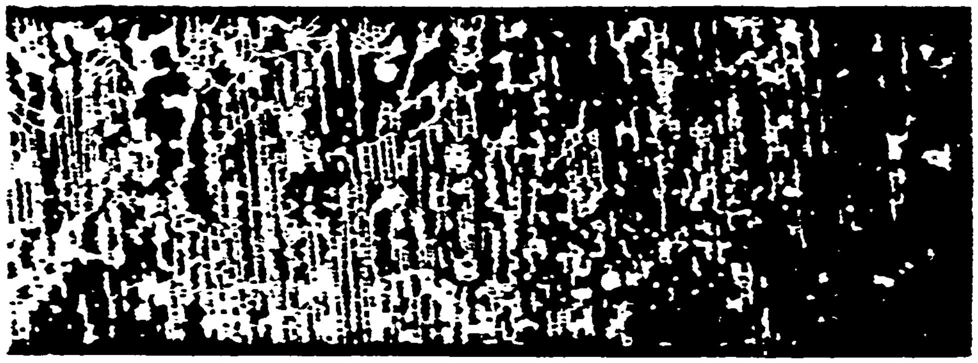

3/8"

a. 950 F diffusion treatment - electroless nickel-plated specimen N5.

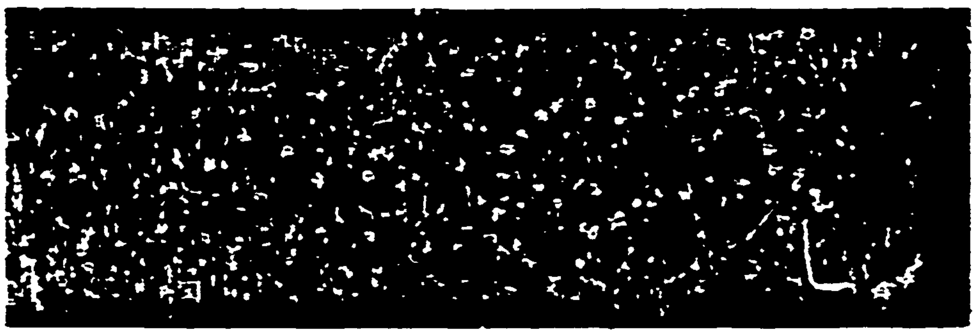

3/8"

b. 1150 F diffusion treatment - electroless nickel-plated specimen E5.

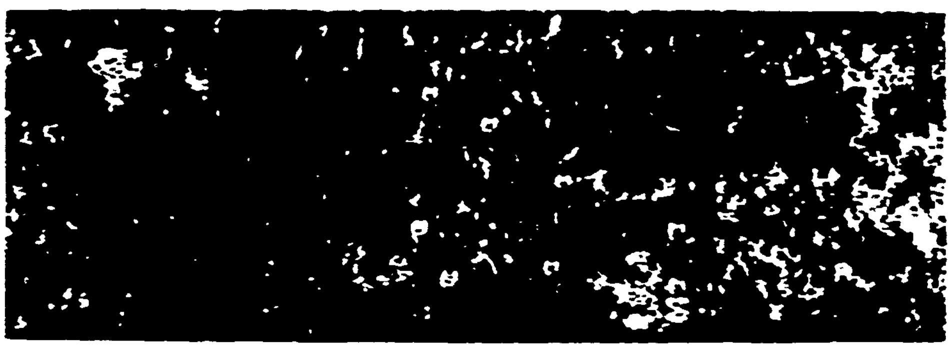

3/8"

c. 1150 F heat treatment - nonplated Ti-5Al-2.5Sn specimen E7.

Figure 11. 1000-hour test at 900 F - salt-treated longitudinal specimens - etched - oblique lighting.

times. Review of the topography of the corroded surfaces revealed that most pits proliferated along strain lines, eventually conjoining to form troughs. Some pits remained isolated and merely increased in diameter. One dominating characteristic which appeared to distinguish troughs and pits from cracks was depth of penetration. Inward growth of the pits and troughs seemed to terminate in the vicinity of the plate-substrate interface, thereby alluding to the sacrificial nature of the electroless nickel plating on titanium.

The earlier observation that the diffusion bond treatment temperatures affected the hot salt failure modes of the electroless nickel plating was confirmed by the specimen appearances after 1000 hours. A comparison of photographs in Figures 11a and 11b succinctly reveals the distinct differences in the characteristics of the corrosion troughs. Corrosion attack of the 950 F treated plate is characterized by the presence of wider-gap troughs possessing a greater propensity to conjugate with other pits and troughs as compared to the 1150 F treated plate.

Also exhibited in the photographs is the controlled influence of the punch marks on the flow of the strain lines as manifested by curvature of the troughs in the vicinity of the cavities. Further, despite the possible rupture and thinning of the plate within the punch cavities, there appeared to be little or no corrosion present. Perusal of the right side of the same figures also reveals some preferential corrosion patterned along the induced diagonal scratch lines. But this phenomenon does not dominate the failure mode thereby indicating the uncertainty of their influence as either stress raisers or harmful plating defects.

For baseline comparison, Figure 11c shows the appearance of the corrosion pit and crack-laden surface on a nonplated Ti-5Al-2.5Sn alloy specimen which was heat treated to conform with the 1150 F diffusion treatment process of one of the platings investigated. Examination of a corresponding 950 F heat-treated, nonplated titanium specimen revealed it to be more resistant to stress corrosion cracking. Since the stress-relief effects should be less at the lower heat treat temperature and since no major changes were observed in the microstructure shown in Figure 1, the cause of this anomaly remains to be studied further.

Substrate Examination

The manifestation of cracks in the surface of the salt-treated platings implies the susceptibility of the electroless nickel plating to HSSCC. Figure 12a shows the appearance of cracks in one segment of 1000-hour specimen E6 under normal lighting conditions. This same specimen was shown earlier in Figure 7a, at a lower magnification. In order to ascertain the extent of damage to the substrate engendered by the corrosion pits, troughs, and cracks in the plate surface, approximately 1-1/2 mils of the top layer was mechanically removed. (The original thickness of the virgin plate was about 0.6 mil.) As evidenced by Figure 12b, the readily identifiable surface cracks had indeed propagated deep into the titanium alloy substrate, while the pits and troughs disappeared with no signs of their original superposition. Figure 12c exhibits the hot salt damage to a typical nonplated titanium specimen.

Embrittlement of the plated surface concomitant with tensile stresses above some unidentified threshold level appear to be the necessary combination for the initiation of cracks. In the segment shown in Figure 12b, it may be noted that, with one exception, the cracks are selectively present at the specimen edge or into a punch-mark cavity which are regions of higher stresses. The single crack shown which was not located at either of those high stress areas may have initiated at the site of a corrosion pit.

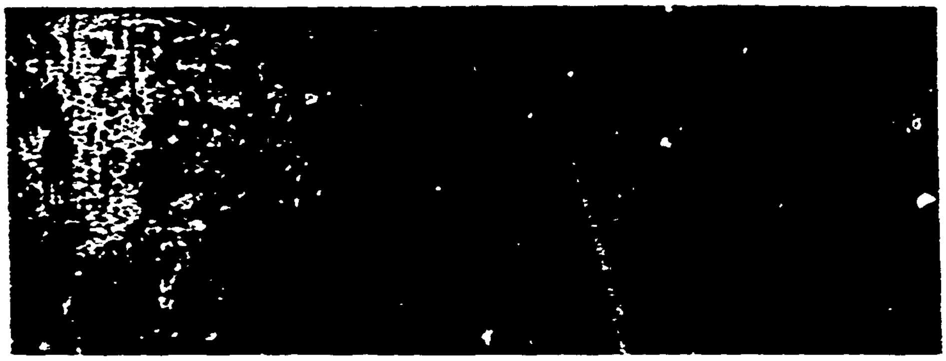

a. Electroless nickel-plated surface specimen E6

b. Ti-5Al-2.5Sn alloy substrate - plating removed specimen E6.

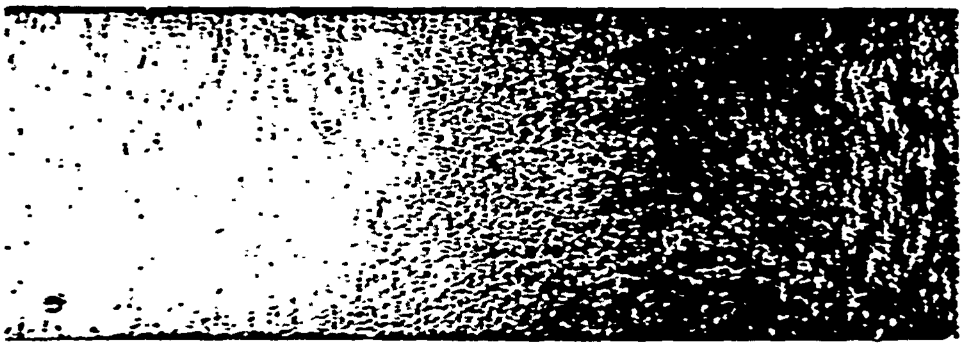

c. Nonplated Ti-5Al-2.5Sn surface specimen E8.

Figure 12. 1000-hour test at 900 F - 1150 F diffusion treatment - [illegible] - treated - etched - transverse specimens. Mag. 5X

Thus, an inference may be drawn that at this test temperature an increase in surface tensile stresses will encourage the initiation of new cracks. However, the relative importance of surface embrittlement versus stress raisers and plating strength in contributing to crack initiation remains undetermined.

Despite the existence of stress raisers at the base of the corrosion troughs, the inward intrusion of corrosive activity was generally arrested at the substrate level. Figure 13 shows a representative damaged cross-section of the electroless nickel plate of specimen N5 after exposure at 900 F for 1000 hours. Apparently, the combination of temperature, corrosive media, and stress in the segments shown were not sufficient to initiate or propagate into the substrate. Although delamination also occurred between diffusion layers of the nickel plate, the base of the diffusion-bonded plate remained firmly attached to the titanium substrate.

Figure 13. 1000-hour test at 900 F - cross-section of salt-treated electroless nickel plate, specimen N5, showing troughs and delaminations. Mag. 1000X

Metallic deposits on the surface of titanium alloys can either promote or inhibit the corrosion process, depending on its electronegativity relative to the substrate.[11] A plating less electronegative than the substrate would be anodic relative to the substrate and thus would tend to corrode preferentially. This reaction would inhibit the stress corrosion process because oxygen reduction would occur at the substrate. On the other hand, if the sacrificial corrosion of the plate encouraged the formation of corrosion products susceptible to hydrolysis, the substrate could still be embrittled by the subsequent formation of nascent hydrogen. In this investigation, the chemical reactions causing the troughs in the plate did not appear to yield by-products adequate for embrittling the substrate sufficiently to cause crack initiation at the stress levels present.

General Comments

As mentioned in earlier statements, titanium alloys are susceptible to hot salt stress corrosion cracking. Observations by previous investigators[11-13] indicate that the substrate is embrittled by the stress corrosion process, eliminating simple dissolution as the failure mode, with the embrittling species being generated by the corrosion process. Moreover, embrittlement by hydrogen is generally accepted as a primary cause of cracking. However, disagreements still exist concerning the mechanism of hydrogen generation. Nevertheless, surface cracking does occur and can be quite severe as previously shown by the representative photographs in Figures 7b, 8, 10a, and 12c.

11. GARFINKLE, M. *Electrochemical Model for Hot Salt Stress-Corrosion of Titanium Alloys.* Metallurgical Transactions, v. 4, July 1973, p. 1677-1685.
12. American Society for Testing and Materials. *Stress-Corrosion Cracking of Titanium,* a Symposium, Special Publication No. 397, Philadelphia, 1966.
13. STAEHLE, R. W., et al. *Fundamental Aspects of Stress Corrosion Cracking.* National Association of Corrosion Engineers, Houston, 1969, p. 591-700.

Cracks and incipient cracks were also present in the surface of the plated specimens after as early as 150-hour exposure time at 900 F, albeit limited in crack quantity (Figure 9) as compared to nonplated titanium specimens (Figure 8). However, in contrast to the random distribution of cracks in the nonplated specimens, the cracks in the plate appeared to be concentrated in regions of higher stress, i.e., edge and cavity peripheries.

The cracks seem to co-exist independent of the corrosion pits and troughs. Hence, it can be speculated that a higher average tensile stress than that employed in this experiment would have promoted the initiation of more surface cracks.

One significant characteristic of the surface cracks in the electroless nickel plating was their continuity into the titanium substrate. Figure 14 shows a cross-section of such a crack. The primary cause of crack initiation in the plated surface was not identified, but embrittlement may be a source. A crack in the plating combined with other reactions, may then encourage the diffusion of harmful chemical species to the substrate forming a crevice where surface embrittlement and cracking of the titanium surface commences to occur. Yet, it is generally recognized that the presence of cracks or stress raisers alone have only a minimal effect on hot salt stress cracking to the extent that precracked test specimens are not useful in these HSSCC experiments. Also, as described earlier, the existence of scratches and indentations in the surface of the plating did not enhance stress corrosion of the exposed areas. Moreover, the pits, troughs, and mechanically induced indentations and scratches did not appear to act as preferential sites for crack initiations.

A representative corrosion crack penetration into the titanium alloy substrate is shown in Figure 15. Propagation of this type of crack has been attributed by Garfinkle[11] to the reaction of titanium with chlorine ions to form a chlorotitanate which hydrolyzes with H_2O to release chlorine ions and TiO_2 along with nascent hydrogen (H^+) which serves as the source of embrittlement in anodic regions such as grain boundaries:

$$Ti + 6Cl^- \rightarrow TiCl_6^= + 4e^-$$

$$TiCl_6^= + 2H_2O \rightarrow TiO_2 + 6Cl^- + 4H^+$$

Combining these reactions, the overall reaction becomes:

$$Ti + 2H_2O \rightarrow TiO_2 + 4H^+ + 4e^-$$

External tensile loads separate the weakened bonds causing the crack to propagate. Absorbed moisture from the surface continues to migrate (capillarity) to the crack tip, re-establishing the anode and chemical reactions. The intergranular nature of the stress corrosion cracks observed in this study is typified by the crack profile exhibited in the micrograph, Figure 16, of the region surrounding the tip of the crack shown in the previous figure. However, the fracture mode is quite dependent upon the solution treatment temperature. In Ti-5Al-2.5Sn alloys treated above the beta transus (1925 F), cracking can be expected to be predominantly transgranular.

The results of this exploratory investigation demonstrated the potential of diffusion-bonded electroless nickel plating as an effective means for protecting

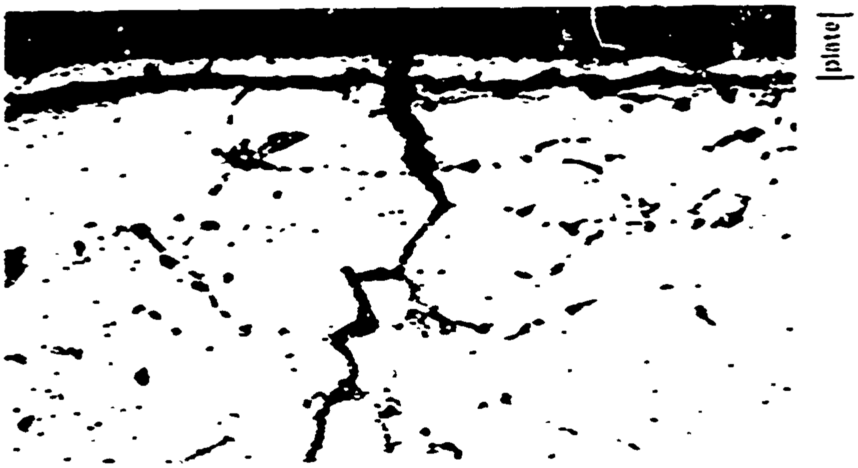

Figure 14. Cross-section of crack through electroless nickel plate layer and Ti-5Al-2.5Sn substrate, specimen E5. Mag. 1000X

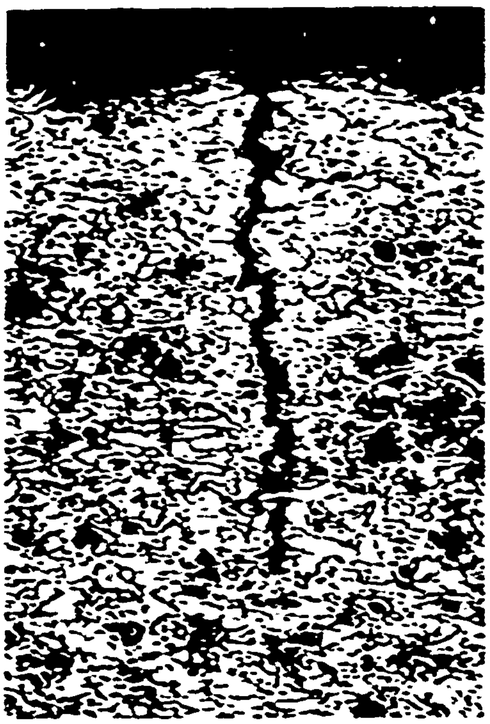

Figure 15. Cross-section view of SC crack penetrating into titanium substrate, specimen E5. Mag. 200X

Figure 16. Enlarged view of region around crack tip showing intergranular penetration into titanium substrate, specimen E5. Mag. 1000X

titanium alloys from the debilitating attack of hot salt stress corrosion. However, the data is valid only within the constraints of this study. Further efforts to optimize the plating (e.g., diffusion treatment time and temperature, composition, plating thickness) and evaluate its limitations is contingent upon satisfactory results from other investigations of the ability of electroless nickel-coated titanium to meet other requirements of gas turbine compressor components, such as fatigue and erosion resistance at elevated temperatures.

CONCLUSIONS

1. Diffusion-bonded electroless nickel plate on titanium alloys can retard hot salt stress corrosion cracking of titanium alloys at 900 F.

2. Minor mechanical defects in the surface of the plating and sheet orientation had little influence on the course of stress corrosion cracking.

3. Diffusion treatment temperatures can affect the stress corrosion behavior of the titanium substrate.

4. Influence of numerous test variables remains to be elucidated. These include composition and condition of titanium substrate, plate parameters including composition, diffusion temperature and thickness, and environmental conditions such as salt composition and density, moisture, oxygen content, air velocity, state-of-stress, temperature, and exposure duration. Mechanisms of failure must be established.

5. Continued efforts to optimize and evaluate electroless nickel plates on titanium alloys for gas turbine compressor component applications are contingent upon satisfactory erosion and fatigue behavior at elevated temperatures.